Mon. Not. R. Astron. Soc. **000**, 000–000 (0000) Printed 19 July 2000 (MN LaTeX style file v1.4)

Compton-thick X-ray absorption in the Seyfert galaxies Tololo 0109–383 and ESO 138–G1

M.J. Collinge* and W.N. Brandt

Department of Astronomy & Astrophysics, The Pennsylvania State University, 525 Davey Lab, University Park, PA 16802, USA (collinge@astro.psu.edu and niel@astro.psu.edu)

19 July 2000

ABSTRACT

We present analyses of the *ASCA* X-ray spectra of two Seyfert galaxies, Tololo 0109–383 and ESO 138–G1. In both cases, spectral fitting reveals two statistically acceptable continuum models: Compton reflection and partial covering. Both spectra have strong iron Kα lines, with equivalent widths greater than 1.5 keV. These large equivalent widths are suggestive of heavier obscuration than that directly indicated by the partial-covering models ($\approx 2 \times 10^{23}$ cm^{-2}), with the actual column densities being 'Compton-thick' (i.e. $N_{\rm H} \gtrsim 1.5 \times 10^{24}$ cm^{-2}). We use the hard X-ray/[O III] flux correlation for Seyferts and data from the literature to provide additional support for this hypothesis. Since Tololo 0109–383 is known to have optical type 1 characteristics such as broad Balmer line components and Fe II emission, this result marks it as a notable object.

Key words: galaxies: individual: Tololo 0109–383 – galaxies: individual: ESO 138–G1 – galaxies: nuclei – galaxies: Seyfert – X-rays: galaxies.

1 INTRODUCTION

The issue of absorption in Seyfert nuclei is one that has motivated a great deal of research. For example, studying the absorbing gas in Seyfert 2s offers the most straightforward means for learning about the putative molecular torus surrounding the central engine, which is a cornerstone of the unified model for Seyferts (e.g. Antonucci 1993). These studies are also pertinent to research aiming to discover the source of the cosmic X-ray background radiation. In both of these cases, a key issue is to understand the distribution of absorbing column densities of the Seyfert population. A recent study by Risaliti, Maiolino & Salvati (1999) reported that roughly half of Seyfert 2s have 'Compton-thick' intrinsic absorption columns ($N_{\rm H} \gtrsim \sigma_{\rm T}^{-1} = 1.5 \times 10^{24}$ cm^{-2}), a fraction that is higher than indicated by earlier studies that were biased toward bright X-ray sources. Since the number of known and well-studied Compton-thick Seyferts is not large, the study of new nearby examples is significant. In this paper, we present a study of two Seyferts, Tololo 0109–383 (NGC 424) and ESO 138–G1, in which we find evidence for the presence of Compton-thick nuclear absorption. ESO 138–G1 is a Seyfert 2 (e.g. Alloin et al. 1992). Tololo 0109–383 was originally classified as a Seyfert 2 as well (Smith 1975), but later studies (Boisson & Durret 1986; Durret & Bergeron 1988; Murayama, Taniguchi & Iwasawa 1998) cast this into doubt. Based on the presence of a broad Balmer line component and Fe II emission lines in its optical spectrum, Murayama et al. (1998) argued for the type 1 nature of Tololo 0109–383, settling on a marginal classification between type 1 and type 2. One of our goals in this study is to use its X-ray properties to gain insight into its actual nature.

Table 1. Basic source properties.

Object	V	z	Galactic $N_{\rm H}$
Tololo 0109–383	13.9	0.012	1.8×10^{20} cm^{-2} [a]
ESO 138–G1	14.3	0.0091	1.6×10^{21} cm^{-2} [b]

[a] Stark et al. (1992) [b] Heiles & Cleary (1979)

Both Tololo 0109–383 and ESO 138–G1 are relatively nearby (see Table 1) and display the so-called coronal lines, high-ionization forbidden optical emission lines from species such as [Fe VII], [Fe X], and [Fe XIV] (Alloin et al. 1992; Murayama et al. 1998). Tololo 0109–383 is interesting in that it is one of only a few known galaxies in which the coronal line region has been observed to be spatially extended. In this study, however, we concern ourselves strictly with these galaxies' X-ray emission and their optical characteristics (such as [O III] λ5007 emission) as they relate to their

* NASA-supported undergraduate research associate.

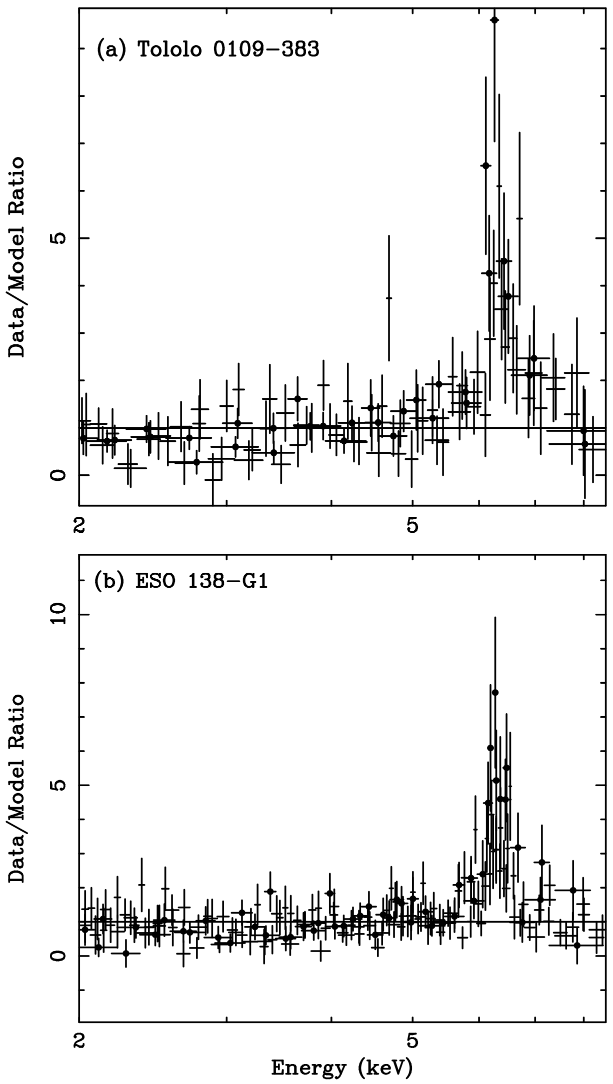

Figure 1. Plots of Model A data-to-model ratio for (a) Tololo 0109–383 and (b) ESO 138–G1. Note the strong residuals due to iron Kα emission from 6–7 keV. Dots are SIS data points, and plain crosses are GIS data points.

X-ray properties. We adopt $H_0 = 70$ km s^{-1} Mpc^{-1} and $q_0 = \frac{1}{2}$.

2 X-RAY OBSERVATIONS AND ANALYSIS

2.1 Observations and data reduction

The *ASCA* observations of Tololo 0109–383 and ESO 138–G1 were performed on 2–3 July 1997 and 6–7 September 1997, respectively. For our analysis, we used Revision 2 processed data from Goddard Space Flight Center, prepared using standard screening criteria (Pier 1997). After screening, the respective SIS/GIS exposure times were 34 ks/34 ks for Tololo 0109–383 and 27 ks/31 ks for ESO 138–G1. For both objects, we utilized XIMAGE (Giommi, Angelini & White 1997) to locate the sources in the SIS and GIS images. We made use of XSELECT (Ingham & Arnaud 1998) to reduce the data.

2.2 Spectral analysis

In order to permit χ^2 fitting, we adopted a minimum spectral group size of 15 events per data point. For the SIS/GIS detectors, we have included the energy ranges 0.6–10 keV/0.9–10 keV. We performed simultaneous fitting of the spectra from all four detectors for each object, and we constrained all parameters to be the same for each group, aside from the absolute model normalizations. We report all equivalent widths and fluxes from the SIS0 detector, and all errors at the 90% confidence level unless otherwise indicated. We have used XSPEC (Arnaud 1996) for all spectral fitting. See Table 2 for a summary of the χ^2 fitting.

We began by fitting the spectra of both objects with a simple power law absorbed by the Galactic column density (Model A). We have allowed for uncertainties of up to 20% in the Galactic column densities; such variations do not materially alter our results. Model A fails to provide a statistically acceptable fit for either spectrum. As shown in Figure 1, there are strong line-like residuals above 6 keV in both spectra. In addition, the photon indices are significantly flatter than expected for intrinsic Seyfert spectra ($0.99^{+0.16}_{-0.14}$ for Tololo 0109–383 and $0.55^{+0.12}_{-0.13}$ for ESO 138–G1). In Model B, we constrained the photon index of the power law to lie in the canonical range for Seyferts; specifically, we required it to be above 1.6 (e.g. Brandt, Mathur & Elvis 1997). We also added a Gaussian emission line to represent iron Kα emission. We constrained the line width parameter σ to lie below 0.4 keV in order to remain consistent with known Seyfert characteristics (e.g. Nandra et al. 1997). The fit improves somewhat for Tololo 0109–383 and is comparable to Model A for ESO 138–G1 (see Table 2); neither is statistically acceptable. Our next step was to add an intrinsic absorption column (Model C), but the best-fit value of this column density is zero for Tololo 0109–383, and therefore the fit does not improve. The improvement in the fit of the spectrum for ESO 138–G1 is slight.

We were able to achieve statistically acceptable fits of both spectra using models consisting of absorption by the Galactic column densities of Compton-reflected continua ('pexrav') plus iron lines (Model D). This type of model is often found to represent well the spectra of absorbed Seyferts. Because of the poor signal-to-noise of our data, we constrained the element abundances to be solar, and we fixed the power-law cutoff energy to be far outside the *ASCA* band at 1000 keV. In Table 3 we list the relevant fit parameters. The high values of the reflection scaling factors indicate that reflected components dominate both spectra, and the photon indices, although poorly constrained, are consistent with reasonable values. We note that the ≈ 6.4 keV lines are consistent with neutral iron Kα emission and that the statistical degradation of the fit is not large if we constrain the line in the spectrum of Tololo 0109–383 to be narrow ($\sigma = 0.05$ keV).

Statistically acceptable fits can also be achieved using models consisting of power laws plus iron lines absorbed by the Galactic column densities and partial-covering (intrinsic) absorption columns (Model E). Like reflection models, partial covering is also often found to be important in the spectra of Seyferts with obscuration. The photon indices and line equivalent widths obtained from this model are consistent with those obtained from Model D, and again the line

Table 2. Model statistics.

Object Name	Parameter	Model A	Model B	Model C	Model D	Model E	Model F
Tololo 0109–383	χ^2/DOF	288 / 171	208 / 171	208 / 171	164 / 171	158 / 171	190 / 171
	$1 - P(\chi^2 \mid \nu)$[a]	5.0×10^{-13}	9.5×10^{-3}	8.2×10^{-3}	0.44	0.54	5.0×10^{-2}
ESO 138–G1	χ^2/DOF	434 / 289	434 / 289	412 / 289	288 / 289	281 / 289	376 / 289
	$1 - P(\chi^2 \mid \nu)$	8.3×10^{-30}	1.2×10^{-8}	4.4×10^{-7}	0.34	0.46	6.8×10^{-5}

[a] $P(\chi^2 \mid \nu)$ is the probability that the observed chi-square for a correct model should be less than a value χ^2 (Press et al. 1989).

Table 3. Best-fit Model D parameters with 90% ($\Delta\chi^2 = 2.71$) errors, X-ray fluxes, and [O III] fluxes.

Parameter[a]	Tololo 0109–383	ESO 138–G1
Refl. scaling factor	88^{+120}_{-14}	70^{+130}_{-32}
Photon index (Γ)	$2.3^{+0.2}_{-0.2}$	$2.1^{+0.4}_{-0.4}$
Line energy (keV)	$6.43^{+0.09}_{-0.10}$	$6.36^{+0.05}_{-0.05}$
Line width (σ) (keV)	$0.20^{+0.28}_{-0.12}$	$0.07^{+0.09}_{-0.07}$
Equivalent width (keV)	$1.6^{+0.4}_{-0.5}$	$1.7^{+0.4}_{-0.4}$
$F^{\rm b}_{0.6-2}$	2.0×10^{-13}	1.8×10^{-13}
$F^{\rm b}_{2-10}$	1.2×10^{-12}	1.8×10^{-12}
$F^{\rm c}_{[\rm O\ III]}$	2.3×10^{-13}	9.3×10^{-13}

[a] All fluxes are reported in erg cm^{-2} s^{-1}. [b] SIS0 observed 0.6–2 keV and 2–10 keV fluxes. [c] [O III] λ5007 emission, corrected for Galactic extinction. From Murayama et al. (1998) and Schmitt & Storchi-Bergmann (1995), respectively. The value reported for ESO 138–G1 is the total flux within 5″ of the nucleus.

energies and widths are consistent with neutral, narrow iron Kα emission. We shall later discriminate between Models D and E based on physical arguments.

As a means of checking the general robustness of these results, we also considered alternate models consisting of Raymond-Smith plasma components added to Model C (Model F). Physically the plasma component represents thermal gas emission such as is often associated with starburst activity (e.g. Ptak et al. 1999). For each spectrum, the fit is a significant improvement over Model B; however, the fits are still not statistically acceptable.

3 DISCUSSION AND CONCLUSIONS

3.1 The iron Kα lines and variability

Iron Kα lines are produced through the reprocessing of primary X-rays and become strongest in equivalent width when the primary X-ray continuum is suppressed in the neighborhood of 6.4–6.97 keV. The large iron Kα equivalent widths (greater than 1.5 keV) and flat apparent spectral continua (see Section 2.2) that we observe in Tololo 0109–383 and ESO 138–G1 indicate that reprocessing is important in these sources (e.g. Matt, Brandt & Fabian 1996), a deduction which seems to be confirmed by the good fits of the spectra that we achieved using Compton-reflection models (Model D). The large reflection scaling factors in those fits indicate that the reflected components dominate any direct components of the nuclear emission to a great extent. We achieved equally good fits, however, using partial-covering

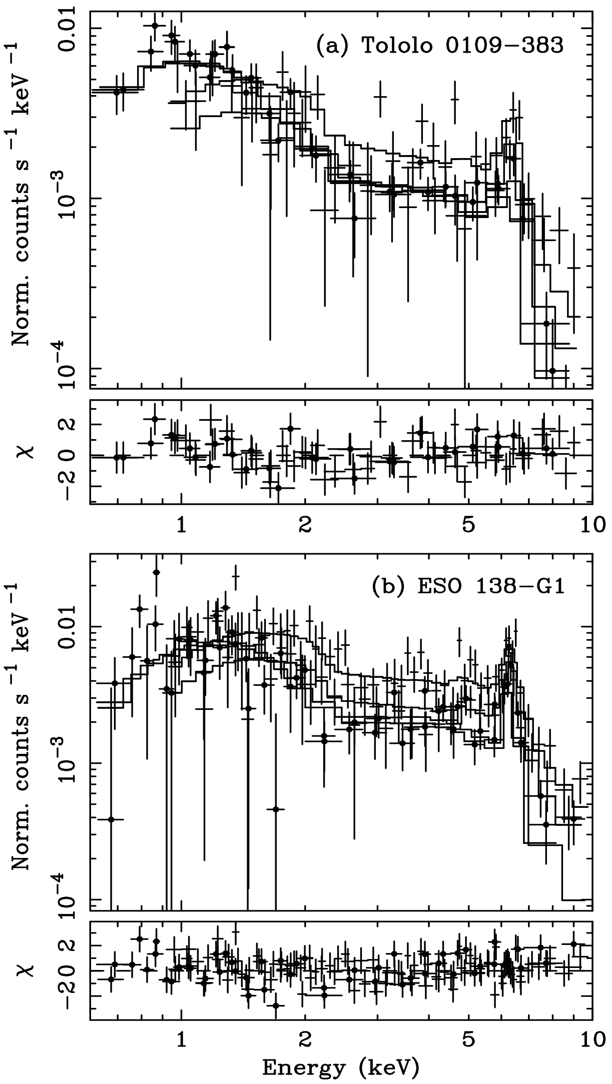

Figure 2. *ASCA* SIS (dots) and GIS (plain crosses) spectra of (a) Tololo 0109–383 and (b) ESO 138–G1. Model D has been fit to the data. The ordinates for the lower panels (labeled χ) show the fit residuals in terms of sigmas with error bars of size one.

models. We must therefore discriminate between the two models based on physical arguments.

Matt et al. (1996) describe two reprocessing mechanisms that can be significant in Seyferts, both of which can produce very strong iron Kα emission. In the first case, the iron emission occurs at the inner surface of the circumnuclear absorbing material (the putative torus). The viewing

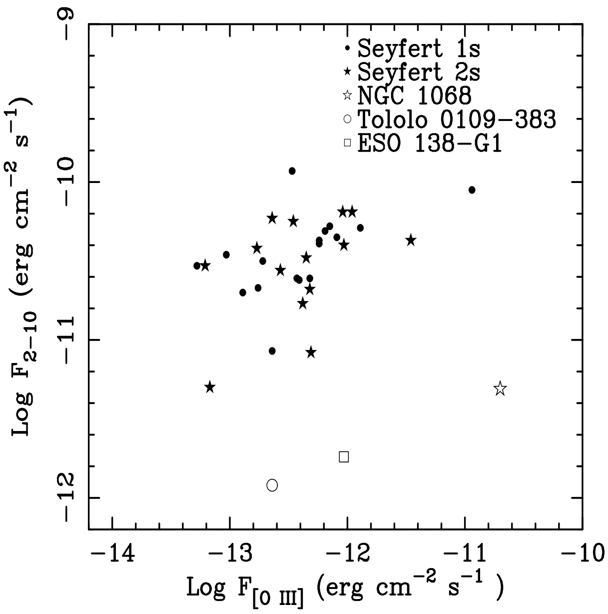

Figure 3. F_{2-10} versus $F_{[\mathrm{O\ III}]}$ for the Seyferts in the Mulchaey et al. (1994) sample plus Tololo 0109–383 and ESO 138–G1. We have updated the 2–10 keV flux for NGC 4051 (a Seyfert 1) using the average flux reported by Guainazzi et al. (1996). The object in the lower right-hand corner, NGC 1068, is a well-known Compton-thick Seyfert 2 (e.g. Matt et al. 1997).

angle can be such that the central source is obscured but the inner wall of the torus is not. In this case, predominantly neutral emission is expected and iron Kα equivalent widths can be up to a few keV. Our Model D is entirely consistent with this theoretical mechanism. The second scenario places the iron emission in optically thin gas in the nuclear region (the 'warm mirror'). As long as the direct X-ray emission is obscured, the iron Kα equivalent width can be as high as a few keV, but in this case the line is expected at higher energies (6.7–6.97 keV), representing emission from very highly ionized iron. If we interpret the partial-covering column densities as representing absorbing gas along some lines of sight through the scattering regions, our Model E is consistent with this scenario, *except for the energies of the iron Kα lines.* These energies are inconsistent at greater than the 90% confidence level with emission from the highest ionization states of iron. Thus we can conclude that a scattered component is not highly significant in the spectra of either Tololo 0109–383 or ESO 138–G1.

Based on these considerations, it is likely that we are primarily seeing reprocessing by the inner surface of a circumnuclear absorber (torus). In order to get the large equivalent widths we observe (greater than 1.5 keV), however, an absorption column density is required that is significantly larger than the intrinsic column densities indicated by Model E. A column density of 2×10^{23} cm^{-2} (of the order we fit in Tololo 0109–383 and ESO 138–G1) absorbs only $\approx 25\%$ of the X-ray flux at 6.4 keV. To get such a large equivalent width in the 6–7 keV range, the intrinsic absorption along a direct line of sight to the X-ray source must be essentially Compton-thick (e.g. Matt et al. 1996).

We have also analyzed *ROSAT* data for Tololo 0109–383 and ESO 138–G1 in order to check for flux variability between the *ROSAT* and *ASCA* observations of these objects. Tololo 0109–383 was observed by the *ROSAT* PSPC on 2–3 July 1992 (Rush & Malkan 1996), and ESO 138–G1 appears in the *ROSAT* HRI field of SN1990W, which was observed on 11–12 September 1995. Hence the variability timescales we are probing are roughly 5 years and 2 years, respectively. Significant low-energy variability would place a constraint upon the size of the scattering/reflecting regions. Based on our analysis of the data and the $F_{0.1-2}$ for Tololo 0109–383 quoted by Rush & Malkan (1996), however, we find no evidence for significant variability between the *ROSAT* and *ASCA* observations of either source. The fluxes are consistent to within the cross-calibration uncertainties of the detectors (e.g. Iwasawa, Fabian & Nandra 1999).

3.2 Additional evidence for Compton-thick absorption

We now consider additional evidence supporting the conclusion that the primary nuclear sources in Tololo 0109–383 and ESO 138–G1 are completely obscured in the *ASCA* band. Mulchaey et al. (1994) reported correlations between $F_{[\mathrm{O\ III}]}$ (see Table 3) and F_{2-10} for Seyferts. They found the following relationships (the reported error ranges are one standard deviation):

$$\log(F_{[\mathrm{O\ III}]}/F_{2-10}) = -1.89 \pm 0.50 \quad \text{(Seyfert 1s)}$$
$$\log(F_{[\mathrm{O\ III}]}/F_{2-10}) = -1.76 \pm 0.62 \quad \text{(Seyfert 2s)}$$

A simple calculation using the fluxes from Table 3 yields the values $\log(F_{[\mathrm{O\ III}]}/F_{2-10}) = -0.72$ for Tololo 0109–383 and $\log(F_{[\mathrm{O\ III}]}/F_{2-10}) = -0.29$ for ESO 138–G1. These numbers fall well outside the 1σ and 2σ ranges, respectively, of even the Seyfert 2 relationship (see Figure 3). This provides further support for the obscuration of most of the direct X-rays from these sources below 10 keV, strengthening the conclusion that the intrinsic absorption in these galaxies is Compton-thick. To emphasize this point, we have used the Seyfert 2 relationship to predict F_{2-10} for the two galaxies from $F_{[\mathrm{O\ III}]}$ (e.g. Turner et al. 1997), and we compare these to the observed values of F_{2-10}. Using the Table 3 fluxes, we obtain values of 11^{+35}_{-8} for Tololo 0109–383 and 30^{+94}_{-23} for ESO 138–G1 for the ratios of predicted to observed fluxes. We note that this is a somewhat conservative estimate for Tololo 0109–383, to which we might also justifiably apply the Seyfert 1 relationship.

3.3 Tololo 0109–383, a Compton-thick type 1 Seyfert

Although the optical properties of Tololo 0109–383 support a Seyfert 1 or intermediate nature (see Section 1), its inferred absorption column density and iron Kα line are more like those of Seyfert 2s. It seems clear that in the case of this object, the simplified picture of a type 1 or type 2 nature falls somewhat short of the truth. Nevertheless, we argue that Tololo 0109–383 is a Compton-thick Seyfert; this seems to be the only plausible explanation for its observed X-ray properties. The combination of its type 1 optical properties with this heavy intrinsic absorption marks it as a member of a peculiar class of objects. It may well serve as a nearby archetype for the heavily obscured type 1 objects recently found in deep X-ray surveys (e.g. Comastri et al. 2000; also see Brandt, Laor & Wills 2000). As we have only placed a lower limit on the intrinsic absorption column in this object, we point out that the remaining uncertainty in its actual value should be resolvable by an observation further into the hard X-ray band by a satellite such as *BeppoSAX*. Finally, we comment that the existence of type 1 objects with heavy X-ray obscuration, such as Tololo 0109–383 and Broad Absorption Line QSOs (e.g. Gallagher et al. 1999), should give pause to those who would classify an object as type 2 based solely on a hard X-ray spectrum.

ACKNOWLEDGMENTS

We gratefully acknowledge financial support from NASA grant NAG5-7256 and the Barry M. Goldwater Scholarship and Excellence in Education Foundation (MJC) and NASA LTSA grant NAG5-8107 (WNB). We thank the referee, Giorgio Matt, for constructive comments. This research has made use of data obtained through the High Energy Astrophysics Science Archive Research Center Online Service, provided by NASA's Goddard Space Flight Center.

After this paper was submitted, we learned that Matt et al. (2000) have confirmed the Compton-thick nature of the absorber in Tololo 0109–383 using data from *BeppoSAX*.

REFERENCES

Alloin D., Bica E., Bonatto C., Prugniel P., 1992, A&A, 266, 117
Antonucci R. R. J., 1993, ARA&A, 31, 473
Arnaud K.A., 1996, in Jacoby G., Barnes J., eds, Astronomical Data Analysis Software and Systems V: ASP Conference Series # 101. ASP Press, San Francisco, p. 17
Boisson C., Durret F., 1986, A&A, 168, 32
Brandt W. N., Laor A., Wills B. J., 2000, ApJ, 528, 637
Brandt W. N., Mathur S., Elvis M., 1997, MNRAS, 285, L25
Comastri A., Fiore F., Vignali C., La Franca F., Matt G., 2000, in Plionis M., Georgantopoulos I., eds., Large Scale Structure in the X-ray Universe. Atlanti Sciences, Santorini, p. 227
Durret F., Bergeron J., 1988, A&AS, 75, 273
Gallagher S. C., Brandt W. N., Sambruna R. M., Mathur S., Yamasaki N., 1999, ApJ, 519, 549
Giommi P., Angelini L., White N., 1997, The XIMAGE Users' Guide: Version 2.53. NASA/GSFC, Greenbelt
Guainazzi M., Mihara T., Otani C., Matsuoka M., 1996, PASJ, 48, 781
Heiles C., Cleary M. N., 1979, Aust. J. Phys. Asrophys. Suppl., 47, 1
Ingham J., Arnaud K., 1998, The XSELECT Users' Guide. NASA/GSFC, Greenbelt
Iwasawa K., Fabian A. C., Nandra K., 1999, MNRAS, 307, 611
Matt G., Brandt W. N., Fabian A. C., 1996, MNRAS, 280, 823
Matt G. et al., 1997, A&A, 325, L13
Matt G., Fabian A. C., Guainazzi M., Iwasawa K., Bassani L., Malaguti G., 2000, MNRAS, in press (astro-ph/0005219)
Mulchaey J. S., Koratkar A., Ward M. J., Wilson A. S., Whittle M., Antonucci R. J., Kinney A., Hurt T., 1994, ApJ, 436, 586
Murayama T., Taniguchi Y., Iwasawa K., 1998, ApJ, 115, 460
Nandra K., George I. M., Mushotzky R. F., Turner T. J., Yaqoob T., 1997, ApJ, 477, 602
Pier E. A., 1997, *ASCA* Getting Started Guide for Revision 2 Data: Version 6.1. NASA/GSFC, Greenbelt
Press W. H., Flannery B. P., Teukolsky S. A., Vetterling W. T., 1989, Numerical Recipes in Pascal. Cambridge University Press, Cambridge
Ptak A., Serlemitsos P., Yaqoob T., Mushotzky R., 1999, ApJS, 120, 179
Risaliti G., Maiolino R., Salvati M., 1999, ApJ, 522, 157
Rush B., Malkan M. A., 1996, ApJ, 456, 466
Schmitt H. R., Storchi-Bergmann T., MNRAS, 276, 592
Smith M. G., 1975, ApJ, 202, 591
Stark A. A., Gammie C. F., Wilson R. W., Bally J., Linke R. A., Heiles C., Hurwitz M., 1992, ApJS, 79, 77
Turner T. J., George I. M., Nandra K., Mushotzky R. F., 1997, ApJ, 488, 164

This paper has been produced using the Royal Astronomical Society/Blackwell Science LaTeX style file.